ISSN 0001-4338, Izvestiya, Atmospheric and Oceanic Physics, 2017, Vol. 53, No. 9, pp. 1185–1191. © Pleiades Publishing, Ltd., 2017.
Original Russian Text © A.V. Polyakov, Yu.M. Timofeyev, Ya.A. Virolainen, A.B. Uspensky, F.S. Zavelevich, Yu.M. Golovin, D.A. Kozlov, A.N. Rublev, A.V. Kukharsky, 2016, published in Issledovanie Zemli iz Kosmosa, 2016, No. 5, pp. 71–78.

RUBRICS

Satellite Atmospheric Sounder IRFS-2
1. Analysis of Outgoing Radiation Spectra Measurements

A. V. Polyakov[a], *, Yu. M. Timofeyev[a], Ya. A. Virolainen[a], A. B. Uspensky[b], F. S. Zavelevich[c], Yu. M. Golovin[c], D. A. Kozlov[c], A. N. Rublev[b], and A. V. Kukharsky[b]

[a]*Saint Petersburg State University, St. Petersburg, Russia*
[b]*State Research Center Planeta, Moscow, Russia*
[c]*State Scientific Centre Keldysh Research Centre, Moscow, Russia*
**e-mail: a.v.polyakov@spbu.ru*

Received June 9, 2015

Abstract—The outgoing radiation spectra measured by the IRFS-2 spectrometer onboard Meteor-M no. 2 satellite have been analyzed. Some statistical parameters of more than 10^6 spectra measured in spring in 2015 have been calculated. The radiation brightness temperature varied from ~300 K (surface temperature) up to
1 ~210 K (tropopause temperature). The quite high variability of the longwave measured radiation has been demonstrated. The signal-to-noise ratio distinctively decreases in the shortwave region (higher than 1300 cm^{-1}). Intercomparisons of IR sounders IRFS-2 with IASI and CrIS spectra showed that the discrepancies in the average spectra and their variability do not exceed measurement errors in the spectral region 660–1300 cm^{-1}. A comparison of specially chosen pairs of the simultaneously measured spectra showed that the differences between IRFS-2 and European instruments in the region of the 15-μm CO_2 band and the transparency windows 8–12 μm are less than 1 mW/(m^2 sr cm^{-1}) and no more than the differences between the two IASI instruments (-A and -B). The differences between measured and simulated spectra are less than 1 mW/(m^2 sr cm^{-1}) in the mean part of CO_2 band. However, starting from 720 cm^{-1}, values appear that reach 2–4 mW/(m^2 sr cm^{-1}). This is caused by the absence of precise information about the surface temperature. Further investigations into the possible reasons for the observed disagreements are required in order to improve both the method of initial processing and the radiative model of the atmosphere.

Keywords: thermal radiation, IR radiation, satellite sounding of the atmosphere, Fourier spectroscopy, Fourier spectrometry

DOI: 10.1134/S0001433817090249

INTRODUCTION

The idea of using measurements of the outgoing thermal radiation of the Earth for a remote determination of vertical atmospheric temperature profiles was first expressed in the 1950s (e.g., Kaplan, 1959). The first space experiments on the implementation of the spectral method of temperature sounding from space were successfully carried out on the Nimbus-3 meteorological artificial Earth satellite (MAES) in 1969 (Wark, Hilleary, 1969; Hanel, Conrath, 1969). In the USSR, the first experiments on the thermal sounding of the atmosphere were carried out in 1971 (Pakhomov et al., 1971). Numerous theoretical and experimental studies of the remote method were carried out further, as well as hardware development, one of the main objectives of which was the fulfillment of sufficiently strict requirements for the accuracy and vertical resolution of satellite sounding of temperature profiles (Uspenskii, 2013; Bondur, Krapivin, 2014; Smith et al., 2009).

A new Russian meteorological satellite Meteor-M No. 2 was launched in July 2014, which carried a variety of equipment for remote sensing (RS) of the atmosphere and Earth's surface, including the IRFS-2 Fourier spectrometer designed to obtain information about the atmosphere and surface for numerical weather forecasts and a study of contemporary climate changes on Earth (Asmus et al., 2014). The main technical characteristics of the IRFS-2 Fourier spectrometer are given in Table 1 (Zavelevich et al., 2009; Golovin et al., 2013).

The IRFS-2 equipment is close to the known IASI devices (Chalon et al., 2001) and CrIS (http://www.ipo.noaa.gov, 2011) in regards to its purpose and basic characteristics. Based on the main field of application of these devices and a sufficiently high spectral resolution, they are usually called hyperspectral IR sounders in domestic and foreign literature.

To interpret the spectra of outgoing radiation of the Earth measured by IRFS-2 sounder, the methods, algorithms, and software–mathematical support for

Table 1. Main technical parameters of the IRFS-2

Parameter	Value
Operating spectral region, μm (cm^{-1})	5–15 (660–2000)
Spectral resolution (unapodized), cm^{-1}	0.4
Noise equivalent power of the spectral brightness, NESR(ν), $mW/(m^2\ sr\ cm^{-1})$	0.1–0.3
Swath, km	1000–2500
Step of spatial grid, km	60–110
Spatial resolution in nadir, km	30
Informativeness, Kb/s	600
Mass of the instrument, kg	50
Operating energy consumption, W	50

processing the IRFS-2 data were developed. On the basis of numerical simulation, the accuracy characteristics of the IRFS-2 measurements were studied in detail and the errors of thematic processing—vertical temperature profiles, humidity, ozone and a number of greenhouse gases, and land and ocean temperatures (Polyakov et al., 2009, 2014)—were estimated. This article is devoted to the results of the first important stage: analysis of the quality of the spectra of outgoing thermal radiation of the atmosphere–surface system measured by the IRFS-2 IR-spectrometer.

SPECTRA OF OUTGOING THERMAL RADIATION OF THE EARTH

Figure 1a (the color version of all figures for this article is presented at the link http://troll.phys.spbu.ru/Personal_pages/Polyakov/color_figures_IKFS_1.docx) shows some statistical characteristics of the outgoing radiation intensity spectra measured by the IRFS-2 instrument in various regions of the globe and with different clouds. The measurements were performed in spring 2015 for ~20 days in the period February 4–April 5. More than 106 spectra were used to obtain these characteristics.

Figure 1a clearly demonstrates the variability of radiation due to changes in temperature and humidity, as well as the presence of clouds and variability of their characteristics in the Earth's atmosphere in the field of view of the device. The maximum values of outgoing thermal radiation are observed in a transparency window of 8–12 μm, in which the ozone absorption band is clearly distinguished near 9.6 μm. The minima of the radiation intensity in this region are related to the low temperatures of the lower stratosphere, and the maximum of the radiation at the center of the band is associated with higher tropospheric temperatures. An interpretation of measurements in this band allows one to determine the total ozone content in the Earth's atmosphere, as well as the details of its vertical distribution. The most transparent regions of the transparency window are used to determine the surface temperature of the oceans, as well as the temperature and emissivity of the land. There is a strong absorption band of CO_2 in the longwave region of 13–15 μm, which is used to determine the vertical temperature profile from the surface of the Earth to the altitudes of 30–40 km. Numerous regions of absorption and radiation by water vapor are used to obtain information on the moisture content of the atmosphere. As was shown in (Polyakov et al., 2010), the measured spectra carry certain information about the content of methane, an important greenhouse gas, and, under certain conditions, other greenhouse gases.

Figure 1b shows the standard deviation and square-averaged measurement errors (the errors vary with time) of the same set of spectra. They clearly demonstrate the relationship between the useful signal—the variability of the recorded radiation intensity—and the noise of the measurements. In particular, it can be seen from the figure that the informativity of the device, which is high in the longwave part of the measured spectrum, decreases significantly in the shortwave region, starting from about 1300–1400 cm^{-1}. This is caused by the use of one receiver in the device, which is relatively insensitive in the shortwave spectral region.

Figure 2 shows examples of the measured spectra in terms of the brightness temperature of the radiation. They clearly demonstrate the spatiotemporal variability of the kinetic temperature of the atmosphere and the surface. This temperature varies in space and spectrum from ~300 K (surface temperature) to ~210 K (tropopause temperature). Variations in the brightness temperature over the spectrum reflect vertical variations in temperature in the troposphere and stratosphere. For example, the minimum brightness temperature in the middle part of the shortwave wing of the 15-μm CO_2 band reflects the temperature at the level of the tropopause, and the maximum of the brightness temperature at the center of the 15-μm band is the temperature of the upper stratosphere.

COMPARISONS OF MEASUREMENT DATA OF IRFS-2 AND IASI IR SENSORS

It is of great interest and practical value to compare the spectra measured by the IRFS-2 with data of similar measurements by instruments currently operating on foreign meteorological satellites. Such comparisons are very important for the mutual calibration of various sounding satellite systems. Figure 3a shows comparisons of the average spectra of outgoing radiation from the atmosphere–surface system for the IRFS-2, IASI-A (European Metop-A satellite), and CrIS (SNPP satellite, United States) devices in the spectral region of the 15-μm carbon dioxide band (660–800 cm^{-1}). These data were obtained on the basis of a large number of individual emission spectra (tens and hundreds of thousands) registered by these instruments on February 5–6, 2015, over the same territory—the Earth's surface from the North Pole to the South Pole—in the same range of observation zenith angles. Note that, for a correct comparison, the spectra of the IASI instrument were reduced to the instrumental function of the IRFS-2 instrument.

Figure 3b shows the differences between the average spectrum of the IRFS-2 from the average spectra of the IASI-B and IASI-A devices in the same spectral region of the 15 μm CO_2 band. The figure shows a high quality of measurements of outgoing radiation spectra by the Russian IR sounder. The difference from the measurements of the European instrument is less than 1 $mW/(m^2\ sr\ cm^{-1})$ and is almost close to the observed difference between the measurements of two IASI instruments (IASI-A and IASI-B). The differences between the average spectra for ITSI-2 and IASI-A are less than 0.4 $mW/(m^2\ sr\ cm^{-1})$ over most of the 15-μm absorption band. We note the maxima of the differences in the regions of the *Q*-branches of the CO_2 band (~667 and ~720 cm^{-1}), where very rapid spectral variations of the absorption coefficients of carbon dioxide are observed. These maxima can be caused by inaccuracies in the coordination of instrumental functions of the devices, which manifest themselves in the region of rapid changes in the intensity of radiation over the spectrum.

It is important that these differences have the same level or even lower than the typical random error of measurements of individual spectra.

The analysis of the mean radiation differences (in terms of brightness temperature) between the IRFS-2 and IASI-A or IASI-B measurements in the spectral range 660–1200 cm^{-1} shows that, for most of the spectral region under consideration, the differences for all three instruments are less than 0.2 K; that is, they are within the limits of the total errors of absolute calibration of these devices. A similar consideration of the spectral region in the transparency window of 8–12 μm shows that the differences in the mean spectra

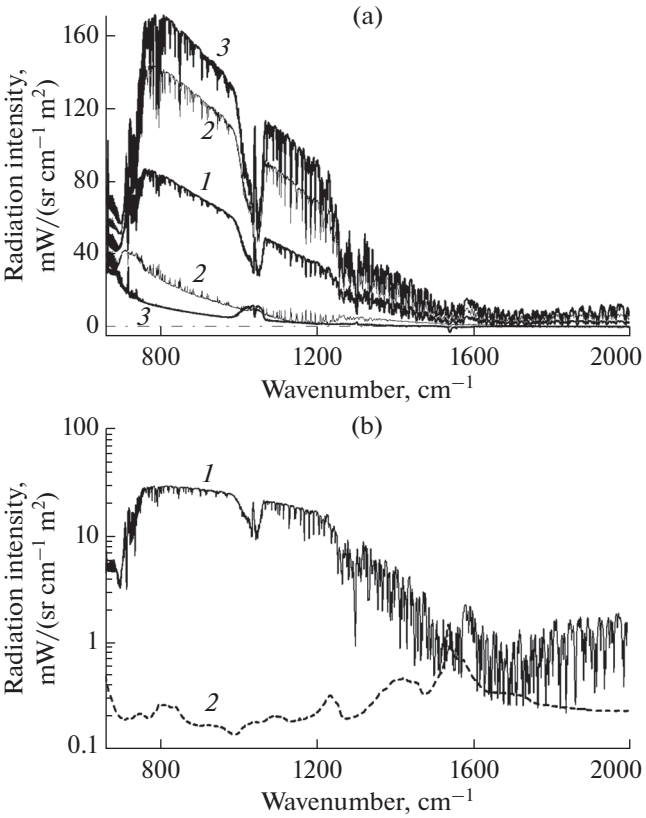

Fig. 1. Statistical characteristics of the spectra of outgoing thermal IR radiation of the atmosphere–surface system measured by the IRFS-2 instrument in different regions of the globe in February–April, 2015: (a) the average spectrum (*1*), "corridor 2," which is the region of the most probable values containing 95% of all data (*2*), minimum and maximum values (*3*); (b) standard deviation of radiation intensity (*1*), root-mean-square error of its measurement (*2*).

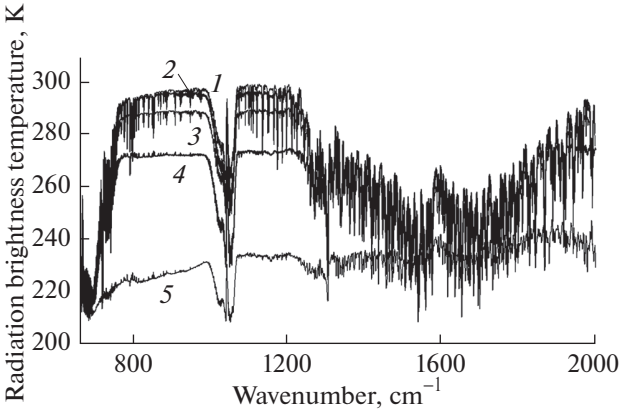

Fig. 2. Examples of spectra of outgoing thermal IR radiation of the atmosphere–surface system in terms of brightness temperature measured by the IRFS-2 instrument in various regions of the world on March 16 and 17, 2015. From the top: Atlantic Ocean near the coast of South America, near the mouth of the Correntine river (*1*); Atlantic Ocean near the coast of Africa (*2*); South Africa, surface altitude of 900 m (*3*); Vsevolozhsky raion, Leningrad oblast (*4*); and Arctic Ocean, 100% cloudiness (*5*).

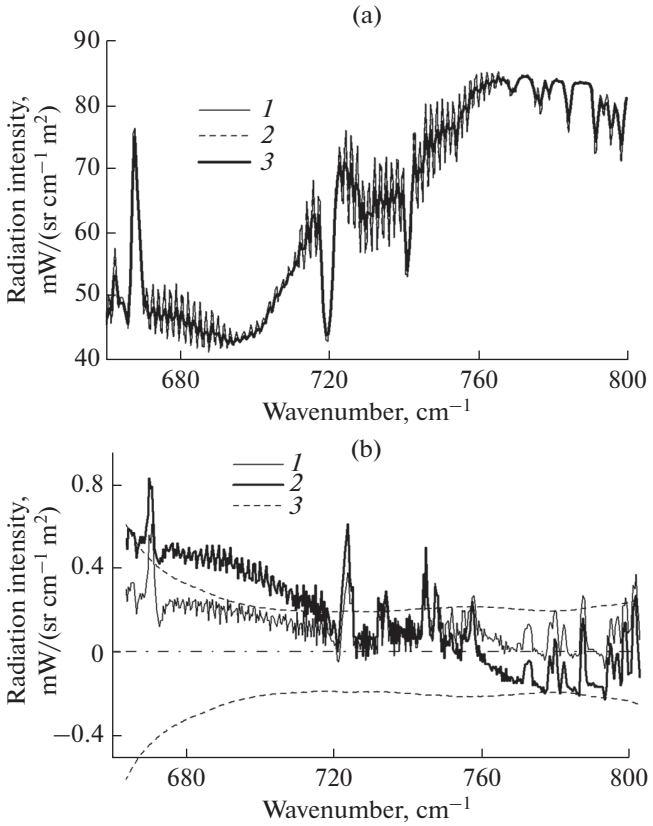

Fig. 3. (a) Comparison of the average outgoing radiation spectra measured by IR sounders (IKFS-2 (*1*), IASI-A (*2*), and CrIS (*3*)) in the spectral region of 15 μm of the carbon dioxide band and a part of the transparency window; (b) differences of the average spectra (IASI-A (*1*) and IASI-B (*2*)) with respect to the IRFS-2 spectra against the background (*3*) of the random error in the IRFS-2 measurements.

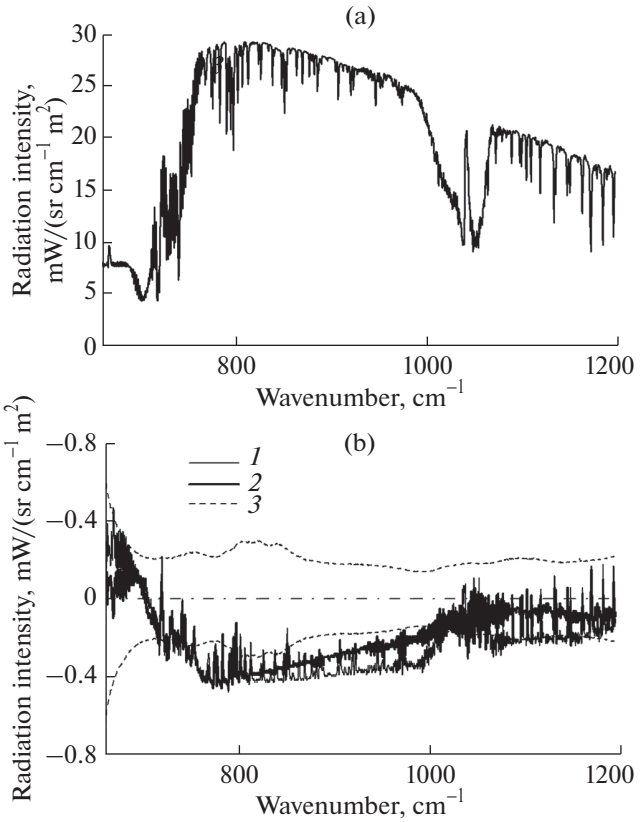

Fig. 4. (a) Standard variations of the outgoing thermal-radiation spectra as measured by the IRFS-2; (b) difference between the standard variations of the outgoing radiation spectra obtained from measurements of IRFS-2, IASI-A (*1*) and IASI-B (*2*); error of IRFS-2 (*3*).

obtained by different instruments do not exceed the random noise of the measurements.

To compare the quality and informativeness of measurements, it is important to compare not only the average spectra, but also the spatial–temporal variations of outgoing radiation measured by various satellite instruments. For the ensembles of spectra measurements described above, standard deviations (natural variations) of outgoing radiation were calculated by different instruments. Figure 4a shows global variations of outgoing thermal radiation from the IRFS-2 measurements, while Fig. 4b shows the difference of variations from the IRFS-2, IASI-A, and IASI-B measurements. In these comparisons, the IASI spectra were reduced to the spectral resolution of the IRFS-2 instrument.

It follows from Fig. 4 that the differences in the recorded natural variations of the outgoing IR radiation by two devices do not exceed 0.5 mW/(m^2 sr cm^{-1}) at the values of these variations reaching 30 mW/(m^2 sr cm^{-1}). This indicates a quite high quality of IR measurements with the IRFS-2 scanner. It should be noted that, given the higher spatial resolution of IASI equipment (~12 instead of ~30 km for the IRFS-2), it is possible to expect slightly higher variability for the spectra recorded by IASI when compared to the IRFS-2 spectra. However, presumably the predominance of homogeneous areas (ocean, steppe, desert, and forest) in the structure of the Earth's surface levels this increase to a slight difference with maximum values of 0.4 mW/(m^2 sr cm^{-1}) in the region of ~800 cm^{-1}. As can be seen, the discrepancies between the mean spectra and the natural variations of the outgoing radiation for various devices are small. This means that all instruments record practically the same spectra of outgoing thermal radiation (in the sense of the first and second moments).

Pairs of the IRFS-2 and IASI-B measurements in cloudless conditions, which have close spacetime coordinates and zenith angles of measurements, were selected for a comparison of individual spectra. The following conditions were met during the selection: the distance between the centers of the pixels of the IRFS and IASI is no more than 20 km, the time difference is no more than 1 h, and the difference in the

zenith angles of the instruments is no more than 2°. The analysis showed that there are systematic differences in the measurements of two instruments in the longwave part of the measurements. The average difference in the spectra obtained by these two instruments in the transparency window is ~1–1.5 mW/(m^2 sr cm^{-1}); there is a region (1200–1400 cm^{-1}) with large chaotic differences reaching 2 mW/(m^2 sr cm^{-1}), and the root-mean-square differences are almost completely determined by the systematic displacement.

COMPARISONS OF MEASURED AND SIMULATED SPECTRA

The accuracy of specifying the radiative transfer model of infrared radiation in the atmosphere (the direct-problem operator), which is used, for example, in the physical–statistical approach for obtaining data of temperature–humidity sounding of the atmosphere (THSA), is of great importance in solving the RS inverse problems (Kondrat'ev, Timofeev, 1978). Numerical simulation of the spectra recorded by the IRFS-2 probe using the integral form of the equation of the intrinsic thermal radiation transfer of the atmosphere–surface system (Timofeev, Vasiliev, 2003) requires specifying various input data such as parameters of physical and optical state of the atmosphere, vertical-temperature profiles, humidity, content of various absorbing gases, aerosols, surface temperature and its emissivity, cloud characteristics, and some characteristics of the satellite equipment. The main source of data on vertical-temperature and humidity profiles is radiosonde measurements. One can also use the results of numerical weather forecasting for this purpose, for example, analysis fields of meteorological element or forecasts with zero lead time. For the numerical simulation of outgoing radiation spectra, the LBLRTM radiation code of polynomial calculations (http://rtweb.aer.com/lblrtm.html) or the fast radiation code RTTOV, adapted to the calculations of the IRFS-2 spectra, was used. It should be noted that the results of comparisons between measured and simulated spectra are significantly affected by errors in measurements of atmospheric parameters, spatial–temporal consistency of the satellite and input data, and by accuracy in specifying the physical and optical characteristics of the surface. To minimize disagreements when comparing satellite and simulated data, only measurements in cloudless conditions were taken. In this case, the emissivity and surface temperature, the data for which were absent, were determined from the spectral measurements themselves.

When selecting pairs of spectra and radiosonde data, the following criteria were used: the distance should be no more than 100 km and the time difference should be no more than 6 h. As a result, a sample of 62 pairs of radiosonde spectra was formed.

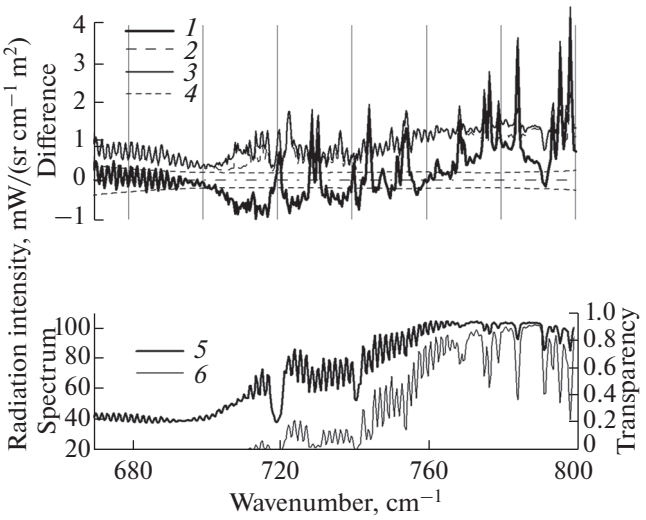

Fig. 5. Comparison of calculated and measured spectra of outgoing IR radiation in the region of 670–800 cm^{-1} (upper panel). Average spectrum and transmission functions of the entire atmosphere (lower panel): mean difference (*1*), standard deviation of the difference (*2*), root-mean-square difference (*3*), measurement error (*4*), typical spectrum (*5*), and typical atmospheric transmission function (*6*).

To complement the profiles above the radiosonde measurement ceiling, the results of the THSA (level 3 data) obtained from the EOS/Aqua satellite information (ftp://acdisc.gsfc.nasa.gov/ftp/data/s4pa/Aqua_AIRS_Level3/AIRX3STD.006/) were used.

Figure 5 shows an example of comparisons of measurements and model calculations in the region of the CO_2 absorption band at 15 μm used for temperature sounding of the atmosphere. The figure shows the mean and root-mean-square differences for a set of comparisons in the region of 670–800 cm^{-1}, as well as (the lower part of the figure) the average spectrum of outgoing thermal radiation and the spectral behavior of the transmission function of the entire atmosphere.

As can be seen from Fig. 5, the average differences in the region of 670–720 cm^{-1} do not exceed ~1 mW/(m^2 sr cm^{-1}); however, starting from 720 cm^{-1}, the maximums having a certain spectral structure appear, which reach 2–4 mW/(m^2 sr cm^{-1}). Further studies and a correction of the radiation model are required to understand and eliminate the causes of the observed differences and their minimization. One of the reasons for the systematic differences in the relatively transparent areas of the CO_2 absorption band may be the errors in setting the carbon dioxide and water-vapor contents in the atmosphere, especially in the troposphere, as well as the errors in determining the emissivity and surface temperature.

The standard deviation of the difference has a more homogeneous spectral structure. It is close to

1 mW/(m^2 sr cm^{-1}) in the center of the 15-μm band and its middle part (660–720 cm^{-1}) (where there is no contribution to the outgoing radiation of the surface; see the lower part of Fig. 5), and gradually increases, reaching ~2 mW/(m^2 sr cm^{-1}) in the wing of the band (720–800 cm^{-1}). We did not analyze the spectral interval 660–670 cm^{-1}, since the radiation in it is formed at altitudes, the data for which are absent in the sources used. As follows from the analysis of the consistency of the calculated and experimental values of the outgoing radiation, further thorough investigations of the causes of these discrepancies are required, as well as the development of techniques for online correction of the direct operator of inverse problem in order to achieve a high accuracy of the THSA results. To solve the first of these tasks, it is extremely important to organize validation programs for remote measurements and complex subsatellite experiments with measurements of numerous physical and optical characteristics of the atmosphere and the surface.

CONCLUSIONS

We considered the results of an analysis of spectra of outgoing infrared radiation measured with high spectral resolution by the domestic IRFS-2 satellite sounder.

Examples of the statistical characteristics of the outgoing radiation intensity spectra measured with the IRFS-2 in different regions of the globe and with different clouds in the spring of 2015 are given. To obtain these characteristics, the period of February 4 to April 5, 2015, was used, and measurements of more than 106 spectra were taken. Quite high radiation variability due to a change in temperature and humidity in the atmosphere, as well as the presence and characteristics of clouds in the Earth's atmosphere in the field of view of the device, is shown. Comparisons of the mean-square natural variations of the outgoing radiation spectra with measurement errors show the high informativeness of the instrument in the longwave measurement region. This informativeness falls noticeably in the shortwave region (more than 1300 cm^{-1}). It seems advisable in the future to add a receiver that is sensitive in the shortwave part of the measurement domain or to exclude the shortwave region, which will reduce noise in the longwave spectral region by introducing a narrower spectral filter.

In terms of the brightness temperature, the radiation spectra demonstrate the spatiotemporal variability of the kinetic temperature of the atmosphere and the surface. This temperature varies in space and spectrum from ~300 K (surface temperature) to ~210 K (tropopause temperature).

We performed a comparison of average spectra of outgoing infrared radiation of the atmosphere–surface system, measured by the IRFS-2, IASI-A and CrIS sounders, and their mean-square (natural) variations obtained from a large number of individual emission spectra (tens of thousands) in February 5–6, 2015, over the same territory (from the North Pole to the South Pole) in the same range of observation zenith angles. The differences in the mean IRFS-2 spectrum from the mean spectra of the IASI-B and IASI-A data (as well as the mean-square variations) do not exceed, as a rule, measurement errors in the spectral region of 600–1300 cm^{-1}. This explains the high quality of measurements of outgoing radiation by the Russian IR sounder. Differences from the measurements of European instruments are less than 1 mW/(m^2 sr cm^{-1}) in the 15-μm region of the CO_2 absorption band and in 8–12 μm transparency window. Practically the same differences are observed between the measurements of the two IASI-A and IASI-B devices.

Comparisons of experimental and simulated spectra of outgoing radiation show discrepancies, the values of which depend on the spectral region. In the center and middle part of the 15-μm band, the CO_2 absorption bands do not, as a rule, exceed ~1 mW/(m^2 sr cm^{-1}). However, starting from 720 cm^{-1}, maxima of differences with a certain spectral structure appear, reaching 2–4 mW/(m^2 sr cm^{-1}). This is probably due to inaccuracies in setting the surface temperature and emissivity. Further analysis of the reasons for the observed differences is required for a possible refinement of both the primary measurement-processing technique and the radiation model. This analysis and possible improvement of the parameters of interaction of radiation and the atmosphere–surface system is planned to be carried out during special programs validating satellite measurements with careful monitoring of the physical and chemical characteristics of this system.

ACKNOWLEDGMENTS

Studies of the quality of the radiation model of the atmosphere in the IR region were carried out at Saint Petersburg State University and were funded by the Russian Scientific Foundation, project no. 14-17-00096. The METEOSAT-10 satellite cloud data and IASI-A and IASI-B measurements on Metop-A and Metop-B satellites provided by EUMETSAT are available on the website https://eoportal.eumetsat.int/. We are grateful to Professor W.L. Smith for providing access to the measurement data of the CrIS device on the SNPP satellite.

REFERENCES

Asmus, V.V., Zagrebaev, V.A., Makridenko, L.A., Milekhin, O.E., Solov'ev, V.I., Uspenskii, A.B., Frolov, A.V., and Khailov, M.N., Meteorological satellites based on Meteor-M polar orbiting platform, *Russ. Meteorol. Hydrol.*, 2014, vol. 39, no. 12, pp. 787–794.

Bondur, V.G. and Krapivin, V.F., *Kosmicheskii monitoring tropicheskikh tsiklonov* (Cosmic Monitoring of Tropical Cyclones), Moscow: Nauchnyi mir, 2014.

Chalon, G., Cayla, F., and Diebel, D., IASI: An advanced sounder for operational meteorology, in *Proceedings of the 52nd International Astronautical Congress of IAF, Toulouse, France, 1–5 October 2001*, Bendisch, J, Ed., 2001.

Clerbaux, C., Boynard, A., Clarisse, L., George, M., Hadji-Lazaro, J., Herbin, H., Hurtmans, D., Pommier, M., Razavi, A., Turquety, S., Wespes, C., and Coheur, P.-F., Monitoring of atmospheric composition using the thermal infrared IASI/MetOp sounder, *Atmos. Chem. Phys.*, 2009, vol. 9, pp. 6041–6054. doi 10.5194/acp-9-6041-2009

Golovin, Yu.M., Zavelevich, F.S., Nikulin, A.G., Kozlov, D.A., Monakhov, D.O., Kozlov, I.A., Arkhipov, S.A., Tselikov, V.A., and Romanovskii, A.S., Spaceborne infrared Fourier-transform spectrometers for temperature and humidity sounding of the Earth's atmosphere, *Izv., Atmos. Ocean. Phys.*, 2013, vol. 50, no. 9, pp. 1004–1015.

Hanel, R. and Conrath, B., Preliminary results from the interferometer experiment on Nimbus III, *Science*, 1969, vol. 165, no. 3899, pp. 1258–1260.

Kaplan, L.D., Inference of atmospheric structure from remote radiation measurements, *J. Opt. Soc. Am.*, 1959, vol. 49, no. 10, pp. 1004–1006. doi 10.1364/JOSA.49.001004

Kondrat'ev, K.Ya. and Timofeev, Yu.M., *Meteorologicheskoe zondirovanie atmosfery iz kosmosa* (Meteorological Sounding of the Atmosphere from Space), Leningrad: Gidrometeoizdat, 1978.

Kondrat'ev, K.Ya. and Timofeev, Yu.M., *Termicheskoe zondirovanie atmosfery so sputnikov* (Thermal Sounding of the Atmosphere from Satellites), Leningrad: Gidrometeoizdat, 1970.

Pakhomov, L.A., Timofeev, Yu.M., Shklyarevskii, V.G., and Pokrovskii, O.M., History of thermal sounding by the Meteor satellite, *Meteorol. Gidrol.*, 1971, no. 11, pp. 5–8.

Polyakov, A.V., Timofeev, Yu.M., and Uspenskii, A.B., Temperature–moisture sounding of the atmosphere by data of IKFS-2, a satellite IR sensing device with high spectral resolution, *Issled. Zemli Kosmosa*, 2009, no. 5, pp. 3–10.

Polyakov, A.V., Timofeev, Yu.M., and Uspenskii, A.B., Possibilities of determination of the content of ozone and other trace gases by data of IKFS-2, a satellite IR sensing device with high spectral resolution, *Issled. Zemli Kosmosa*, 2010, no. 3, pp. 3–11.

Polyakov, A.V., Timofeev, Yu.M., and Virolainen, Ya.A., Using artificial neural networks in the temperature and humidity sounding of the atmosphere, *Izv., Atmos. Ocean. Phys.*, 2014, vol. 50, no. 3, pp. 330–336.

Smith, W.L., Revercomb, H., Bingham, G., Larar, A., Huang, H., Zhou, D., Li, J., Liu, X., and Kireev, S., Technical note: Evolution, current capabilities, and future advances in satellite nadir viewing ultra-spectral IR sounding of the lower atmosphere, *Atmos. Chem. Phys.*, 2009, vol. 9, pp. 5563–5574.

Timofeev, Yu.M. and Vasil'ev, A.V., *Teoreticheskie osnovy atmosfernoi optiki* (Theoretical Foundations of Atmospheric Optics) St. Petersburg: Nauka, 2003.

Uspenskii, A.B. and Rublev, A.N., The current state and prospects of satellite hyperspectral atmospheric sounding, *Izv., Atmos. Ocean. Phys.*, 2014, vol. 50, no. 9, pp. 892–903.

Wark, D.Q. and Hilleary, D.T., Atmospheric temperature: Successful test of remote probing, *Science*, 1969, vol. 165, no. 3899, pp. 1256–1258.

Zavelevich, F.S., Golovin, Yu.M., Desyatov, A.V., Kozlov, D.A., Matsitskii, Yu.P., Nikulin, A.G., Travnikov, R.I., Romanovskii, A.S., Arkhipov, S.A., and Tselikov, V.A., Technological model of the onboard Fourier spectrometer IKFS-2 for temperature–humidity probing of the atmosphere, *Sovrem. Probl. Distantsionnogo Zondirovaniya Zemli Kosmosa*, 2009, vol. 6, no. 1, pp. 259–266.

Translated by I. Ptashnik

SPELL: 1. longwave